Article

Hydrogen Production by Methanol Steam Reforming over CuO/ZnO/Al_2O_3 Catalysts Based on Oxalate-Precursor Synthesis

Haiguang Wang * , Yongfeng Liu , Jun Zhang

Posted Date: 8 September 2023

doi: 10.20944/preprints202309.0550.v1

Keywords: Microwave irradiation; CuO/ZnO/Al2O3 catalyst; Isomorphous substitution; Methanol steam reforming doi:10.20944/preprints202309.0550.v1

ARTICLE

Hydrogen Production by Methanol Steam Reforming over $CuO/ZnO/Al_2O_3$ Catalysts Based on Oxalate-Precursor Synthesis

Haiguang Wang *, Yongfeng Liu and Jun Zhang

School of mechanical-electronic and vehicle engineering, Beijing university of civil engineering and architecture, haidian district, Beijing 100044, China

Abstract: $CuO/ZnO/Al_2O_3$ catalyst is a commonly used catalyst for rea methanol steam reforming reaction. Oxalic acid was as precipitant in preparing oxalate precursor of $CuO/ZnO/Al_2O_3$ catalyst by co-precipitation, deionized water and ethanol were as solvents, microwave irradiation and water bath were as aging heating manner respectively. It indicated that ethanol selected crystal phase composition of oxalate precursors and restricted their growth. Microwave irradiation prompted the isomorphous substitution between Cu^{2+} of CuC_2O_4 and Zn^{2+} of ZnC_2O_4 in mother liquid, forming the master phase $(Cu,Zn)C_2O_4$ in precursor, the solid solution Cu-O-Zn formed after calcination, which exhibited nano-fibriform morphology. It possessed small CuO grains, large surface area and strong synergy between CuO and ZnO, which is beneficial to improve the catalytic performance of methanol steam reforming, the STY of H_2 reached 516.7 $mL\cdot g^{-1}\cdot h^{-1}$, and the selectivity of CO was only 0.29%.

Keywords: microwave irradiation; $CuO/ZnO/Al_2O_3$ catalyst; isomorphous substitution; methanol steam reforming

1. Introduction

Hydrogen energy has been called "the ultimate energy of the 21st century", and there is a huge development space for hydrogen energy. Among various hydrogen production methods, hydrogen production via methanol is increasingly favored by researchers, methanol as a raw material is easy to store and transport [1]. Currently, there are four main ways to produce hydrogen from methanol: methanol decomposition, (MD, equation (1)), partial oxidative reforming of methanol (POM， equation (2)) methanol steam reforming (MSR, equation (3)), and oxidized methanol steam reforming (OSRM, equation (4)), respectively [2].

$$CH_3OH \rightarrow 2H_2 + CO \quad \Delta H = +128.0\ kJ\cdot mol^{-1} \quad (1)$$

$$CH_3OH + 0.5O_2 \rightarrow 2H_2 + CO_2 \quad \Delta H = -192.2\ kJ\cdot mol^{-1} \quad (2)$$

$$CH_3OH + H_2O \rightarrow 3H_2 + CO_2 \quad \Delta H = +49.4\ kJ\cdot mol^{-1} \quad (3)$$

$$CH_3OH + (1-n)H_2O + 0.5nO_2 \rightarrow (3-n)H_2 + CO_2 \quad \Delta H = +49(1-n)-192.2n\ kJ\cdot mol^{-1} \quad (4)$$

Among the four methods of hydrogen production, MSR is the most widely studied and the most in-depth method. MSR produce the highest amount of hydrogen per mole of methanol, and has the advantages of high purity of hydrogen and low content of CO [3]. Besides, MSR technology has low reaction temperature, low energy consumption and low investment [4].

At present, there are two types of catalysts used in MSR for hydrogen production [5,6]: one type is precious metal catalysts (such as Pd/ZnO, etc.); the other type is non-precious metal catalysts, including non-copper based catalysts (such as Zn-Cr, etc.) and copper based catalysts (such as $CuO/ZnO/Al_2O_3$, etc.).

Cu-based catalysts can produce H_2 with high selectively at low temperatures and have low CO selectivity, so Cu-based catalysts are widely used. The Cu-based catalysts for MSR have been widely studied, the effect of synergy between CuO and ZnO and the surface structure of $CuO/ZnO/Al_2O_3$ catalysts on the catalytic activities are critical [7,8].

Co-precipitation is a common method for preparing $CuO/ZnO/Al_2O_3$ catalysts, the precipitation process have a profound impact on the structure and performance of the prepared catalysts. Inui et al. [9] studied the effects of pH and temperature on catalyst precursors in the precipitation process. It indicated that the formation of $Cu_2(NO_3)(OH)_3$ is advantageous when $pH \leq 6$, while $(Cu,Zn)_2CO_3(OH)_2$ is dominant when $pH \geq 7$. The effect of temperature on the precursor is mainly to change the reaction rate, it has almost no effect on its phase composition. Spencer et al. [10] studied the phase transition process in the mother liquor, it indicated that amorphous $Cu_2CO_3(OH)_2$ first generated, which gradually transformed into $(Cu,Zn)_2CO_3(OH)_2$ during the aging process. Fang et al. [11] studied the effects of different feeding methods. $Cu_2(NO_3)(OH)_3$ mainly formed in the forward addition method, while amorphous $Cu_2CO_3(OH)_2$ mainly formed in the concurrent flow method, which interacts with $Zn_5(CO_3)_2(OH)_6$ and transforms into $(Cu,Zn)_2CO_3(OH)_2$ and $(Cu,Zn)_5(CO_3)_2(OH)_6$, respectively, a CuO-ZnO solid solution formed after decomposition, which is the active phase of MSR reaction.

The solvents and heating methods are the main factors in the precipitation process. Ma et al. [12] prepared $CuO/ZnO/Al_2O_3$ catalyst using ethanol and diethylene glycol as solvent, which possessed larger superficial area and exhibit higher catalytic performance. Zhang et al. [13,14] synthesized the smaller particle $CuO/ZnO/Al_2O_3$ catalyst by oxalate co-precipitation using ethanol as solvent, the catalyst showed better catalytic performance for MSR. Dai et al. [15] investigated the surface property of $CuO/ZnO/Al_2O_3$ catalysts prepared by oxalate co-precipitation, and explained that isomorphous substitution promoted synergy between CuO and ZnO and increased the superficial content of CuO.

Microwave irradiation heating was rapid and even in the preparation of catalysts, the active components was well-distributed on the support. Besides, microwave irradiation could control the micro structure of materials and enhance the selectivity of target product [16]. It is reported that microwave irradiation had obvious effects on preparation of ZnO and Al_2O_3 nanoparticles [17]. Zhang et al. [18] treated $CuO/ZnO/Al_2O_3$ catalysts with microwave irritation (200W) for 3 ~ 10 min, the catalyst micro structure was significantly improved and the catalytic activity of MSR increased by 7%. Fernández et al. [19] synthesized CuO/ZnO precursor mainly containing aurichalcite and $CuO/ZnO/Al_2O_3$ precursor only containing hydrotalcite-like, respectively, under microwave irradiation. The aurichalcite was burned into Cu-O-Zn solid-solution, which exhibited strong synergy and exhibited excellent activity and stability in MSR reaction.

At present, researchers generally believe that the strong synergy effect between Cu and Zn is beneficial for hydrogen production via MSR, many direct evidences for the evolution of the structure, morphology and coordination status of Cu-O-Zn solid solution were provided, which lay a foundation for identifying the active sites and studying the interface effect in the catalytic process [20–22].

In present work, the carbonate precursor is replaced by the oxalate precursor, and ethanol replaced water as a solvent, microwave replaced conventional heating as a heating method, the synergy effect between CuO and ZnO was further strengthened. The effects of solvents and heating methods on the composition of oxalate precursors, the structure, properties, and final MSR reaction performance of the calcined catalysts were studied from atomic to nano-scales.

2. Experimental

2.1. Catalyst preparation

The $Cu-O-Zn/Al_2O_3$ catalyst precursors were prepared by dropping simultaneously 1 mol/L $Cu(NO_3)_2-Zn(NO_3)_2-Al(NO_3)_3$ ($Cu^{2+}/Zn^{2+}/Al^{3+} = 16/8/1$ (molar ratio)) solution and 1 mol/L $H_2C_2O_4$

solution into a beaker with stirring constantly and keeping in water bath at 70 °C. Then the suspension was aged in microwave oven or water bath with circulating cooling equipment after co-precipitation, the aging process was conducted at 80 °C for 1 h. The precipitate was filtered and washed with distilled water or ethanol, then the precursor was obtained after drying at 110 °C for 12 h, and the catalyst was obtained after calcining the corresponding precursor at 350 °C for 4 h in air atmosphere. The precursor was designated as XYP and the catalyst was designated as XYC. Table 1 shows the summary the preparation conditions of the catalysts.

Table 1. Summary of the preparation condition of catalysts.

Catalyst	Precursor	Solvent	Heating manner
WWC	WWP	Water	Water bath (WB)
EWC	EWP	Ethanol	Water bath (WB)
WMC	WMP	Water	Microwave irradiation (MI)
EMC	EMP	Ethanol	Microwave irradiation (MI)

2.2. Catalyst characterization

X-ray diffraction (XRD) patterns of solid samples were recorded using a Rigaku D/max 2500 power diffractometer with Cu Kα radiation at 40 kV and 100 mA with a scanning rate of 8°/min in the 2θ ranges from 10° to 40°.

Temperature-programmed reduction (H_2-TPR) was performed in an Autochem Ⅱ 2920. About 20 mg catalyst sample was set in a U-mode quartz tube, pretreated in a Helium at 50 °C for 30 min, then heated to 300 °C at a rate of 10 °C/min, under a mixture of 10 vol% H_2/Ar (50 ml/min), the sample was then heated to 600 °C at a rate of 10 °C /min, The consumption of hydrogen was monitored by a thermal conductivity detector.

Differential thermal gravity (DTG) measurement was executed in a STA409C thermal analyzer. 30 mg sample was heated to 600 °C at a rate of 8 °C/min in a gas mixture of 20 vol% O_2/N_2 (50 ml/min).

JSM-6700F cold-field scanning electron microscope (SEM) was used to characterize the size and morphology of the samples.

BET specific surface areas and pore distribution of catalyst was measured with a SORPTMATIC 1990 automatic adsorption instrument employing N_2 as the adsorbent. BET specific surface areas were calculated by applying the Brunauer-Emmett-Teller (BET) method.

X-ray photoelectron spectroscopy (XPS) spectra of the samples were collected on an ESCAL-ab 220i-XL electron spectrometer using Al Kα radiation at 300 W. The samples were compressed into a pellet of 2 mm thickness and then mounted on a sample holder. The chamber was maintained at lower than 10^{-10} Torr. The binding energies were calibrated by C1s as the reference energy (C1s = 284.6 eV).

2.3. Catalytic performance of MSR

The performance evaluation of MSR was conducted on a continuous flow fixed bed device with a catalyst loading of 2 g, using industrial refined methanol as raw material. Evaluation conditions: raw material methanol aqueous solution (the molar ratio of water to methanol is 1.5), reaction temperature 260 °C, pressure 0.5 MPa, WHSV = 1.0 h^{-1}. After cooling, gas and liquid samples were analyzed using chromatographs equipped with PorpakT columns and TDX-01 columns, respectively,

doi:10.20944/preprints202309.0550.v1

and thermal conductivity cell detectors. The methanol conversion rate and product distribution were calculated.

3. Results and discussion

3.1. XRD characterization of precursors

Figure 1 shows the XRD patterns of all catalyst precursors. It is seen that the phases of $CuC_2O_4{\cdot}xH_2O$ (2θ = 18.5°, 23.1°, 31.2°, 36°, 38.5°), α-$ZnC_2O_4{\cdot}2H_2O$ (2θ = 18.9°, 35.1°), and β-ZnC_2O_4 (2θ = 24°, 25.1°, 29.1°, 34.1°, 36.9°) were observed in precursor of WWP prepared by water solvent and water bath heating. But only diffraction peaks of $CuC_2O_4{\cdot}xH_2O$ (2θ = 23.1°, 36°, 38.5°) and weak peaks of β-ZnC_2O_4 (2θ = 24°, 36.9°) existed in precursor of EWP prepared by ethanol solvent and water bath heating, no α-$ZnC_2O_4{\cdot}2H_2O$ phase was observed. It indicated that ethanol solvent restrained the formation of α-$ZnC_2O_4{\cdot}2H_2O$, and enhanced the phase selectivity of product. Microwave irradiation promoted the isomorphous substitution between Cu^{2+} of $CuC_2O_4{\cdot}xH_2O$ and Zn^{2+} of ZnC_2O_4 in mother liquid, thus, WMP and EMP mainly contained $(Cu,Zn)C_2O_4$ and partial CuC_2O_4 failing to be substituted during aging, so diffraction peak of $CuC_2O_4{\cdot}xH_2O$ (2θ = 23.1°, 36°) and β-ZnC_2O_4 (2θ = 24°, 36.9°) overlapped each other respectively and deviated original position. Compared with WWP and EWP, WMP and EMP didn't contain diffraction peaks of α-$ZnC_2O_4{\cdot}2H_2O$ and β-ZnC_2O_4, and the crystal degree declined and failed to be detected owning to isomorphous substitution, it indicated that microwave irradiation have strong selectivity on the formation of crystal phase [23,24].

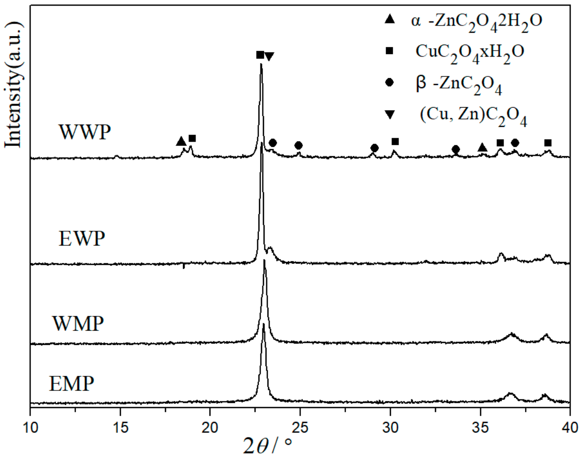

Figure 1. XRD patterns of the catalyst precursors.

$CuC_2O_4{\cdot}xH_2O$, α-$ZnC_2O_4{\cdot}2H_2O$ and β-ZnC_2O_4 generated in mother liquid in co-precipitation, as equation (1), (2) and (3). The isomorphous substitution mainly occurred in the aging process, it means that the Cu^{2+} of CuC_2O_4 entered into ZnC_2O_4 and the Zn^{2+} of ZnC_2O_4 entered into CuC_2O_4 formed $(Cu,Zn)C_2O_4$, as equation (4) and (5). However, the concentration of Cu^{2+} was higher than that of Zn^{2+}, it primarily produced CuC_2O_4 as equation (1) in mother liquid, and the ZnC_2O_4 was little. In other words, the reaction (4) and (5) were promoted simultaneously by microwave irradiation, while CuC_2O_4 was not substituted completely.

$$Cu^{2+} + C_2O_4^{2-} + xH_2O \rightarrow CuC_2O_4{\cdot}xH_2O \qquad (1)$$

$$Zn^{2+} + C_2O_4^{2-} + 2H_2O \rightarrow \alpha\text{-}ZnC_2O_4{\cdot}2H_2O \qquad (2)$$

$$Zn^{2+} + C_2O_4^{2-} \rightarrow \beta\text{-}ZnC_2O_4 \qquad (3)$$

$$CuC_2O_4 + xZn^{2+} \rightarrow (Cu_{1-x},Zn_x)C_2O_4 \qquad (4)$$

$$ZnC_2O_4 + xCu^{2+} \rightarrow (Cu_x,Zn_{1-x})C_2O_4 \qquad (5)$$

3.2. DTG characterization of precursors

DTG curves of different catalyst precursors are shown in Figure 2. Three weight loss peaks for WWP were observed at 118 °C, 308 °C and 343 °C respectively, as shown in equation (6) ~ (9), the peak at 118 °C was due to the desorption of physically absorbed water of α-$ZnC_2O_4{\cdot}2H_2O$, the peak around 308 °C was ascribed to the decomposition of $CuC_2O_4{\cdot}xH_2O$ or $(Cu,Zn)C_2O_4$, and the peak at about 343 °C was attributed to decomposition of β-ZnC_2O_4 and further decomposition of α-ZnC_2O_4 [13]. The weight loss peak for $CuC_2O_4{\cdot}xH_2O$ at 307 °C and weak peak for β-ZnC_2O_4 at 343 °C were observed from curve of EWP, which verified the XRD analysis of its precursor.

$$\alpha\text{-}ZnC_2O_4{\cdot}2H_2O \rightarrow \alpha\text{-}ZnC_2O_4 + 2H_2O \qquad (6)\ t \approx 118\ °C$$

$$CuC_2O_4{\cdot}xH_2O \rightarrow CuO + CO_2 + H_2O \qquad (7)\ t \approx 308\ °C$$

$$\alpha\text{-}ZnC_2O_4 \rightarrow ZnO + CO_2 \qquad (8)\ t \approx 343\ °C$$

$$\beta\text{-}ZnC_2O_4 \rightarrow ZnO + CO_2 \qquad (9)\ t \approx 343\ °C$$

$$(Cu,Zn)C_2O_4 \rightarrow (Cu,Zn)O + CO_2 \qquad (10)\ t \approx 296\ °C$$

WMP and EMP prepared under microwave irradiation only included weight loss peak for $(Cu,Zn)C_2O_4$ or $CuC_2O_4{\cdot}xH_2O$ at about 300 °C, it can be speculated that microwave irradiation accelerated the isomorphous substitution between Cu^{2+} and Zn^{2+}, the lesser Zn^{2+} was incorporated into CuC_2O_4, so there is little content of α-$ZnC_2O_4{\cdot}2H_2O$ or β-ZnC_2O_4 and there were no corresponding decomposition peaks. Especially, EMP had a large quantity of substitution and produced more $(Cu,Zn)C_2O_4$, the crystal phase trended to uniformity, therefore, the decomposition peak of EMP became narrower and the decomposition temperature decreased by 12 °C [23], the peak was mainly ascribe to $(Cu,Zn)C_2O_4$ and partial CuC_2O_4 unable to be substituted as equation (7) and (10).

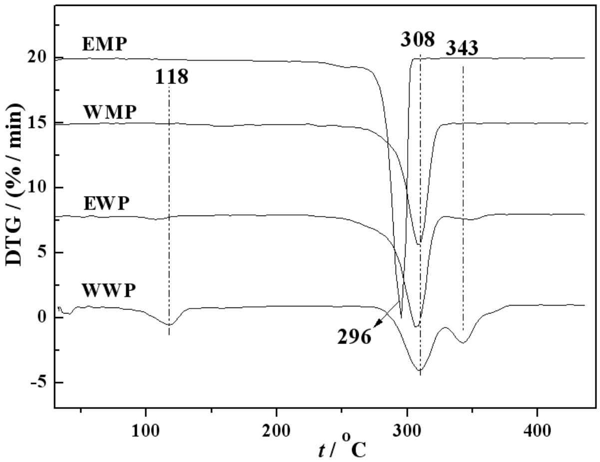

Figure 2. DTG curves of catalyst precursors.

3.3. SEM images of precursors and catalysts

SEM images of different precursors are shown in Figure 3, SEM images of different catalysts after calcining the corresponding precursors ar shown in Figure 4. The appearance of catalysts kept coherence with precursors in some extent by comparing Figure 3 and Figure 4. WWP presented as spherical particles, its diameter was 400 nm or so, it exhibited wafer-shaped and agglomerated each other after calcination, its particle size reduced to 300 nm about. EWC was consisted of irregular bar-shaped and block-shaped, 400 nm in size, it elucidated that ethanol solvent had effects on the shaping process of precursor in mother liquid. EWC didn't change a lot on appearance or size compared with EWP, its size was about 300~400 nm, however, there were many minor porous channel in its superficial structure.

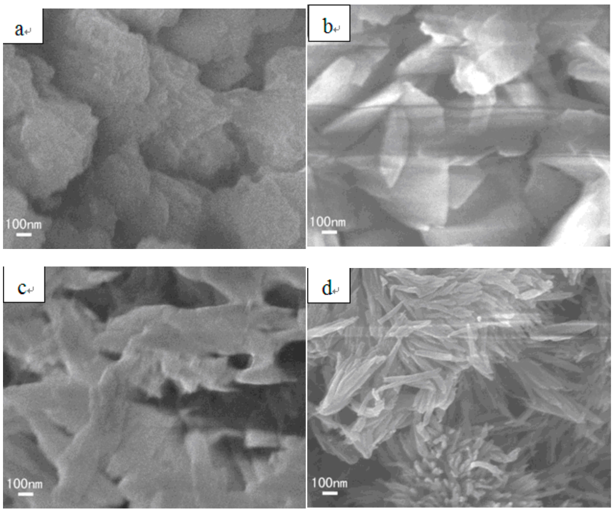

Figure 3. SEM images of catalyst precursors. (a) WWP; (b) EWP; (c) WMP; (d) EMP.

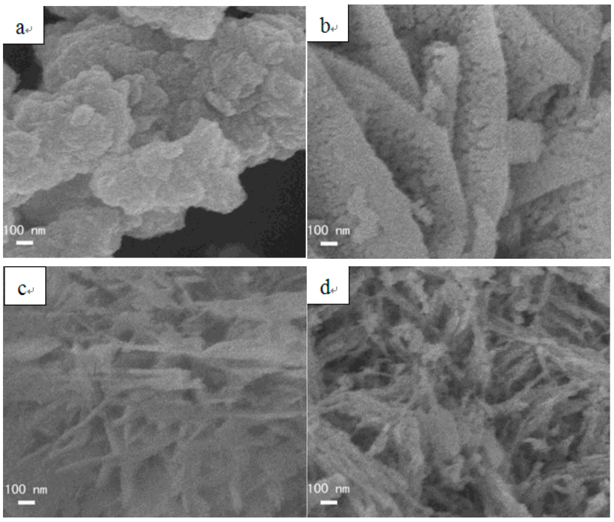

Figure 4. SEM images of catalysts. (a) WWC; (b) EWC; (c) WMC; (d) EMC.

After introducing microwave irradiation, irregular uniwafer could be observed from morphology of WMP, its size was in the range of 300~500 nm. WMC was needle-like and flakiness owning to not be broke down completely, its diameter of section was about 50~100 nm; when ethanol was selected as solvent further, EMP mainly contained unidirectional ordered fibrous nanoparticles, its diameter of section was about 50 nm, which exhibited fine fibrous or flocculent and dispersed evenly after calcination [25].

After combining SEM photographies of precursors and catalysts, it can be concluded that precursors formed towards low dimensions under bulk heating effects of microwave. Precursors prepared by water bath exhibited spherical and massive, while precursors prepared by microwave irradiation presented single fibrous, which particle size was smaller than the former. The particle diameter of EMC was merely 50 nm, it dispersed well and the superficial activity sites distributed evenly, which benefited to improve the catalytic performance of MSR.

3.4. XRD characterization of catalysts

XRD patterns of different catalysts can be seen in Figure 5. The average grain size calculated by Scherrer formula at 2θ ≈ 35.5°, 38.7° and the texture parameters of different catalysts are listed in Table 2. There were no peaks assigned to Al_2O_3 in the four patterns, indicating that Al_2O_3 existed as amorphous or the content of Al_2O_3 was low. Diffraction peaks of CuO appeared in all the four catalysts at 2θ of 38.7°, CuO peaks of WWC were very sharp, the grain size of CuO was comparatively large, up to 18.8 nm as shown in Table 2. The CuO peaks of EWC became smoother when using ethanol as solvent, in which the ZnO peaks at 2θ=34.4°, and 36.3° overlapped with CuO peak at 2θ =35.5°. CuO grain size of EWC reduced to 12 nm, which indicated that viscous ethanol restricted the growth of precursor in mother liquid, resulting in a decrease in CuO grain size after calcination.

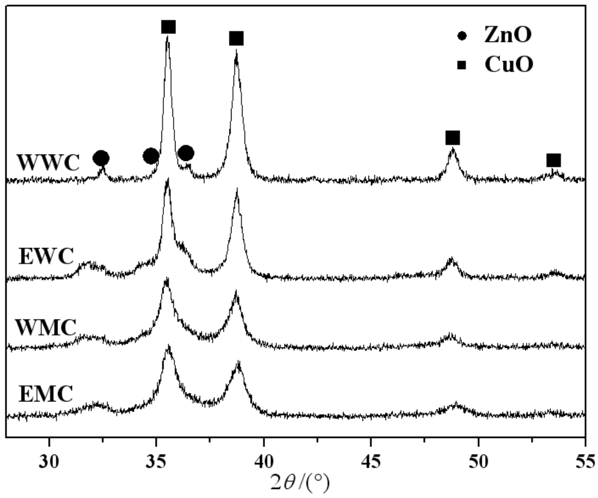

Figure 5. XRD patterns of catalysts.

From patterns of WMC and EMC in Figure 5, it can be observed that the CuO peak becomes smoother, after introducing microwaves. Weak peaks of ZnO could still be seen in WMC, however, no peaks assigned to ZnO were detected in EMC. It indicated that isomorphous substitution took place in mother liquid when microwave irradiation was introduced, partial Cu^{2+} of CuC_2O_4 was incorporated into ZnC_2O_4 and almost all Zn^{2+} of ZnC_2O_4 was incorporated into CuC_2O_4, thereby, the original crystal structure were destroyed and the crystal degree declined after substitution. Cu-O-Zn solid solutions were obtained after calcining WMP and EMP, in which there existed strong synergy between CuO and ZnO. CuO crystal was surrounded averagely by ZnO crystal, which restricted the growth of CuO crystallites, so the grain size of CuO in WMC and EMC were merely 8.9 nm and 8.4 nm respectively [24].

Table 2. Results of grain size and textural properties of catalysts.

Catalyst	Grain size /nm		Textural properties	
	2θ≈35.5°	2θ≈38.7°	Surface area (m^2/g)	Pore volume (cm^3/g)
WWC	18.8	14.4	43.9	0.27
EWC	12.0	13.9	56.4	0.31

WMC	8.9	11.2	59.5	0.29
EMC	8.4	9.5	77.2	0.36

As shown in Table 2, catalysts prepared under microwave irradiation possessed bigger surface area and pore volume than that prepared in water bath, surface area and pore volume of EMC were 77.2 m^2/g and 0.36 cm^3/g respectively. This is because there was much more $(Cu,Zn)C_2O_4$ in precursor prepared under microwave irradiation, the precursor were converted into (Cu,Zn)O (or Cu-O-Zn) solid solution after calcination, in which ZnO and CuO arrayed homogeneously and closely, restricting the agglomeration of CuO, therefore the catalysts were very fine and possessed large surface area. The mother liquid was sol-like after aging when ethanol was selected as solvent, the catalyst possessed large surface area after calcining corresponding precursor [26], so the pore volume of EWC and EMC was comparatively large as shown in Table 2.

3.5. H_2-TPR characterization of catalysts

Figure 6 shows H_2-TPR curves of different catalysts. Ethanol restricted the growth of precurs phase and favored forming fine catalysts which made the reduction process easy. It manifested that reduction temperature of catalysts prepared using ethanol as solvent was lower than that using water. The catalysts prepared by water bath heating were difficult to reduce, the reduction temperature of WWC and EWC was 240 °C approximately, while the reduction temperature of catalysts prepared by microwave irradiation was lower, it was 220 °C or so. It proved again that microwave irradiation selected the phase in the generation process of precursor, the catalyst arranged orderly in micro structure, which decreased the difficulty of reducing CuO by H_2.

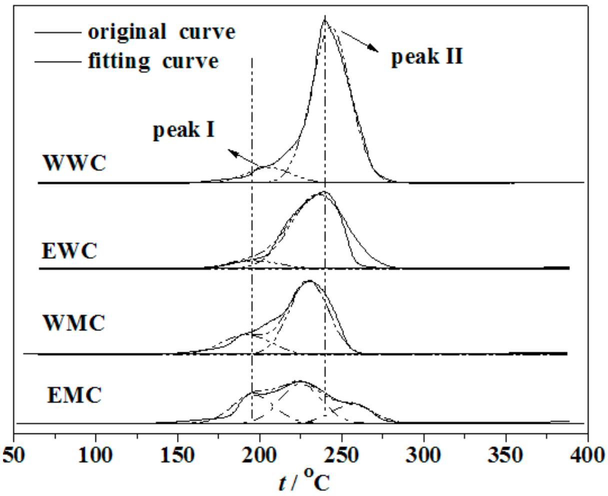

Figure 6. H_2-TPR curves of catalysts.

As shown in Figure 6, one low temperature reduction peak and one high emerged in curves of WWC, EWC, and WMC, however, three peaks emerged in curve of EMC, the first two were divided to low temperature reduction peaks, the third was divided to high temperature reduction peak. Low temperature reduction peaks were assigned to reduction of scattered phase CuO (Peak I), while the other was assigned to reduction of bulk phase CuO (Peak II). The amount of isomorphous substitution was little in mother liquids aging heated by water bath, thus, its synergy between CuO and ZnO was weak and there mainly existed bulk phase CuO in corresponding catalyst, so their Peak II was larger. The amount of substitution between Cu^{2+} and Zn^{2+} was great when aging under microwave irradiation, they mainly generated $(Cu,Zn)C_2O_4$ in precursors which were calcined into Cu-O-Zn solid solutions. The catalysts were homogeneous and dispersive, the synergy was strong, so the Peak I was larger. Especially, the amount of substitution for EMC was great, the reduction peak assigned to high temperature was much smaller than others [27,28].

3.6. XPS and AES characterization of catalysts

XPS spectra of catalysts are shown in Figure 7. As shown in Figure 7(a), all catalysts showed a distinctive BE (binding energy) of Cu $2p_{3/2}$ around 932~933 eV, companying a characteristic satellite peak between 940 ~ 945 eV due to the electron shakeup process, which indicated that Cu species were present as CuO. The BE of Cu $2p_{3/2}$ around 932 ~ 933 eV in spectra of WWC, EWC, WMC and EMC were 932.0 eV, 932.05 eV, 932.10 eV and 932.95 eV respectively, increasing gradually. The BE of Zn$2p_{3/2}$ (Figure 7(b)) in corresponding spectra were 1021.45 eV, 1020.6 eV, 1020.35 eV and 1020.15 eV, decreasing gradually, which were lower than the BE (1022.2 eV) of pure ZnO [29].

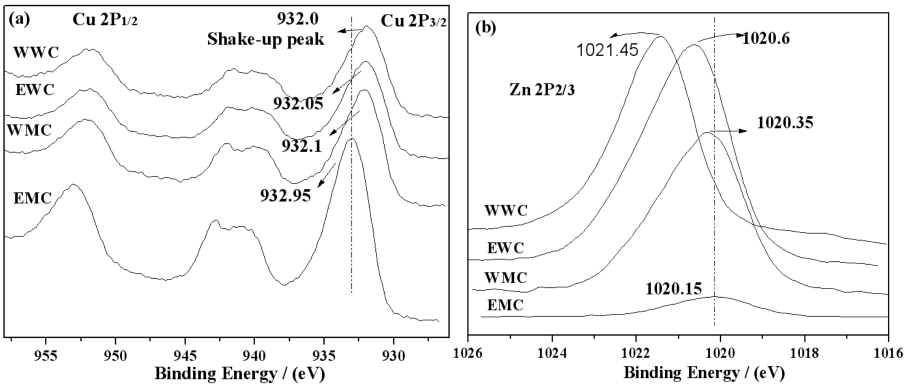

Figure 7. XPS spectra of catalysts.

It illustrated that isomorphous substitution took place when introducing microwave in aging process. The chemical environment and energy status of copper and zinc changed in the gotten Cu-O-Zn solid solution. Because the electronegativity of zinc was higher than copper, the outermost electron of copper shifted towards zinc, the electron density of copper decreased and its binding energy increased, while the electron density of zinc increased and its binding energy decreased [23].

Table 3 lists the data analysis based on XPS and AES spectra and the superficial elements concentration of different catalysts. EMC possessed higher superficial copper content and lower superficial zinc content, its ratio of X_{Cu}/X_{Zn} was up to 8.98, which exceeded all others, it can be verified by the intensity of spectra in Figure 7 and Figure 8. In Table 3, it also could be observed that ethanol solvent help to improve the content of superficial copper atoms. Besides, microwave irradiation raised the yield of (Cu,Zn)C_2O_4 in precursor, leading to lower KE (kinetic energy) of Cu LMM and higher KE of Zn LMM in final catalyst as shown in Figure 8. This was coincident with the research result of literature [15].

Table 3. XPS and AES data of different catalysts.

Catalyst	Surface atom/%			BE(Cu $2p_{3/2}$) /eV	BE(Zn $2p_{3/2}$) /eV	KE(Cu LMM) /eV	KE(Zn LMM) /eV
	Cu	Zn	X_{Cu}/X_{Zn}				
WWC	6.56	15.61	0.42	932.00	1021.45	919.10	988.30
EWC	4.96	9.17	0.54	932.05	1020.60	919.05	988.35
WMC	5.49	8.7	0.63	932.10	1020.35	918.95	988.80
EMC	10.77	1.2	8.98	932.95	1020.15	918.20	988.85

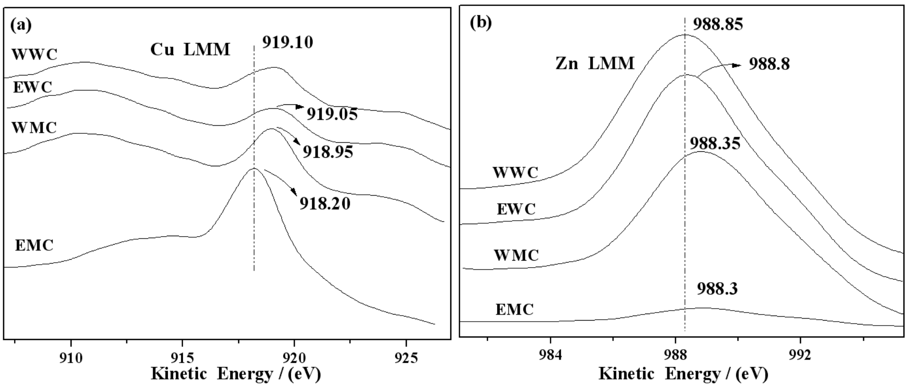

Figure 8. AES patterns of catalysts.

3.7. Catalytic performance test for MSR reaction

The catalytic performance of different catalysts for MSR is listed in Table 4. When comparing WWC and EWC, it can be concluded that ethanol solvent is conducive to reducing the CO selectivity of the catalyst. As can be seen from the XRD data, ethanol optimized precursor crystal phase composition, thereby reducing the CO selectivity. When comparing WWC and WMC, it can be concluded that microwave heating is conducive to improving the methanol conversion rate of the catalyst. As can be seen from the BET data and SEM images, microwave radiation increases the specific surface area of the catalyst, improves the dispersity of copper, increases more active sites, and thus improves the methanol conversion rate. Besides, as can be seen from the XRD data, microwave irradiation prompted the isomorphous substitution between cooper and zinc oxalate precursors, Cu-O-Zn solid solution formed after calcination, which possessed strong synergy and benefited the MSR reaction.

Table 4. Catalytic performance of different catalysts for MSR reaction.

Catalyst	Solvent	^{a}Heating Manner	X_{MeOH} /%	STY_{H2} /mL·g^{-1}·h^{-1}	$^{b}S_{CO}$ /%
WWC	Water	WB	53.6	300.0	1.53
EWC	Ethanol	WB	59.1	333.9	0.39
WMC	Water	MI	85.0	479.5	0.82
EMC	Ethanol	MI	91.2	516.7	0.29

^{a} Evaluation conditions: the molar ratio of water to methanol is 1.5 in the methanol aqueous solution, T = 260 °C, P =0.5 MPa, WHSV = 1.0 h-1. ^{b} WB represents water bath, MI represents microwave irradiation. ^{c} X_{MeOH}： methanol conversion; S_{CO}： CO selectivity.

Thus, it illustrated that both ethanol and microwave irradiation benefited to improve the catalytic performance of MSR, the catalyst EMC prepared by ethanol solvent and microwave heating exhibited optimal catalytic performance, the conversion of methanol was 91.2%, the space time yield (STY) of H_2 reached 516.7 mL·g^{-1}·h^{-1}, its selectivity of CO was only 0.29%; In stark contrast, the catalyst WWC prepared by water solvent and water bath heating showed the worst catalytic performance, its conversion of methanol was only 53.6%, and the STY of H_2 was 300.0 mL·g^{-1}·h^{-1}, but its selectivity of CO was as high as 1.53%.

4. Conclusion

In the preparing process of $CuO/ZnO/Al_2O_3$ catalyst precursors, ethanol solvent selected the crystal phase composition in precursor and restricted its growth. Microwave irradiation promoted the isomorphous substitution between oxalate copper and oxalate zinc, the precursor mainly contain $(Cu,Zn)C_2O_4$ and exhibit nano-fibriform morphology. Either using ethanol as solvent or adopting microwave irradiation as aging heating manner benefited MSR reaction, the catalyst EMC prepared by ethanol solvent and microwave heating showed the optimal catalytic performance, the maximum STY_{H2} reached 516.7 $mL \cdot g^{-1} \cdot h^{-1}$, the conversion of CH_3OH reached 91.2%, and the selectivity of CO was only 0.29%.

Acknowledgments: This study was supported by National Natural Science Foundation of China (21676158), and National Key Research and Development Program (2018A23).

References

1. Kawamura Y, Ogura N, Igarashi A. Hydrogen production by methanol steam reforming using microreactor. J Jpn Petrol Inst 2013;56(5):288-97.
2. Yong ST, Ooi CW, Chai SP, Wu XS. Review of methanol reforming-Cu-based catalysts, surface reaction mechanisms, and reaction schemes. Int J Hydrogen Energ 2013;38(22):9541-52.
3. Xu XH, Shuai KP, Xu B. Review on copper and palladium based catalysts for methanol steam reforming to produce hydrogen. Catalysts, 2017;7(6):183.
4. Iulianelli A, Ribeirinha P, Mendes A, Basile A. Methanol steam reforming for hydrogen generation via conventional and membrane reactors: a review. Renew Sust Energ Rev 2014;29:355-68.
5. Iwasa N, Masuda S, Ogawa N, Takezawa N. Steam reforming of methanol over Pd/ZnO: effect of the formation of PdZn alloys upon the reaction. Appl Catal A: Gen 1995;125(1):145-57.
6. Shokrani R, Haghighi M, Jodeiri N, Ajamein H, Abdollahifar M. Fuel cell grade hydrogen production via methanol steam reforming over $CuO/ZnO/Al_2O_3$ nanocatalyst with various oxide ratios synthesized via urea-nitrates combustion method. Int J Hydrogen Energ 2014;39(25): 13141-55.
7. Shishido T, Yamamoto Y, Morioka H, Takehira K. Production of hydrogen from methanol over Cu/ZnO and $Cu/ZnO/Al_2O_3$ catalysts prepared by homogeneous precipitation: steam reforming and oxidative steam reforming. J Mol Catal A: Chem 2007;268:185-94.
8. Agrell J, Birgersson H, Boutonnet M, Melián-Cabrera I, Navarro RM, Fierro JLG. Production of hydrogen from methanol over Cu/ZnO catalysts promoted by ZrO_2 and Al_2O_3. J Catal 2003;219(2):389-403.
9. Spencer MS. Precursors of copper/zinc oxide catalysts. Catal Lett 2000;66: 255-7.
10. Li JL, Inui T. Characterization of precursors of methanol synthesis catalysts copper/zinc/aluminum oxides precipitated at different pH and temperatures. Appl Catal A: Gen 1996;137: 105-17.
11. Fang DR, Ren WZ, Liu ZM, Xu XF, Xu L, Lv HY, et al. Synthesis and applications of mesoporous Cu-Zn-Al_2O_3 catalyst for dehydrogenation of 2-butanol, J Nat Gas Chem 2009;18(2):179-82.
12. Ma Y, Sun Q, Wu D, Fan WH, Zhang YL, Deng JF. A practical approach for the preparation of high activity $Cu/ZnO/ZrO_2$ catalyst for methanol synthesis from CO_2 hydrogenation. Appl Catal A: Gen 1998;171:45-55.
13. Zhang YL, Sun Q, Deng JF, Wu D, Chen SY. A high activity $Cu/ZnO/Al_2O_3$ catalyst for methanol synthesis: Preparation and catalytic properties. Appl Catal A: Gen 1997;158:105-20.
14. Zhang XR, Wang LC, Yao CZ, Cao Y, Dai WL, He HY, et al. A highly efficient $Cu/ZnO/Al_2O_3$ catalyst via gel-coprecipitation of oxalate precursors for low-temperature steam reforming of methanol. Catal Lett 2005;102:183-90.
15. Dai WL, Sun Q, Deng JF, Wu D, Sun YH. XPS studies of $Cu/ZnO/Al_2O_3$ ultra-fine catalysts derived by a novel gel oxalate co-precipitation for methanol synthesis by CO_2+H_2. Appl Surf Sci 2001;177:172-9.
16. Wu ZJ, Ge SH, Zhang MH, Li W, Tao KY. Synthesis of a supported nickel boride catalyst under microwave irradiation. Catal Commun 2008;9:1432-8.
17. Sule EE, Sadik C, Siddik I. Conventional and microwave-assisted synthesis of ZnO nanorods and effects of PEG400 as a surfactant on the morphology. Inorg Chim Acta 2009;362:1855-8.
18. Zhang XR, Wang LC, Cao Y, Dai WL, He HY, K.N. Fan. A unique microwave effect on the microstructural modification of $Cu/ZnO/Al_2O_3$ catalysts for steam reforming of methanol. Chem Commun 2005;102:4104-6.
19. Fernández Y, Menéndez JA, Arenillas A, Fuente E, Peng JH, Zhang ZB, et al. Microwave-assisted synthesis of CuO/ZnO and $CuO/ZnO/Al_2O_3$ precursors using urea hydrolysis. Solid State Ionics 2009;180:1372-8.
20. Nakamura J, Choi Y, Fujitani T. On the issue of the active site and the role of ZnO in Cu/ZnO methanol synthesis catalysts. Top Catal 2003;22: 277-85.

21. Kasatkin I, Kurr P, Kniep B, Trunschke A, Schlögl R. Role of lattice strain and defects in copper particles on the activity of Cu/ZnO/Al_2O_3 catalysts for methanol synthesis. Angew Chem Int Edit 2007;46(38):7324-7.
22. Behrens M, Studt F, Kasatkin I, Kühl S, Hävecker M, Abild-Pedersen F, et al. The active site of methanol synthesis over Cu/ZnO/Al_2O_3 industrial catalysts. Science 2012;336(6083):893-7.
23. Wang LC, Liu YM, Chen M, Cao Y, He HY, Wu GS, et al. Production of hydrogen by steam reforming of methanol over Cu/ZnO catalysts prepared via a practical soft reactive grinding route based on dry oxalate-precursor synthesis. J Catal 2007;246:193-204.
24. Ning WS, Shen HY, Liu HZ. Study of the effect of preparation method on CuO-ZnO-Al_2O_3 Catalyst. Appl Catal A: Gen 2001;211:153-7.
25. An X, Li JL, Zuo YZ, Zhang Q, Wang DZ, Wang JF. A Cu/Zn/Al/Zr fibrous catalyst that is an improved CO_2 hydrogenation to methanol catalyst. Catal Lett 2007;118:264-9.
26. Bao J, Liu ZL, Zhang Y, Tsubaki N. Preparation of mesoporous Cu/ZnO catalyst and its application in low-temperature methanol synthesis. Catal Commun 2008;9:913-8.
27. Yang RQ, Yu XC, Zhang Y, Li WZ, Tsubaki N. A new method of low-temperature methanol synthesis on Cu/ZnO/Al_2O_3 catalysts from CO/CO_2/H_2. Fuel 2008;87:443-50.
28. Bae JW, Kang SH, Lee YJ, Jun KW. Synthesis of DME from syngas on the bifunctional Cu–ZnO–Al_2O_3/Zr-modified ferrierite: Effect of Zr content, Appl Catal B: Environ 2009;90:426-35.
29. Baltes C, Vukojevi´c S, Schüth F. Correlations between synthesis, precursor, and catalyst structure and activity of a large set of CuO/ZnO/Al_2O_3 catalysts for methanol synthesis. J Catal 2008;258:334-44.